JOURNAL OF BACTERIOLOGY, Feb. 1995, p. 998–1007 Vol. 177, No. 4
0021-9193/95/$04.00+0

Role of Outer Membrane Barrier in Efflux-Mediated Tetracycline Resistance of *Escherichia coli*

DAVID G. THANASSI, GREG S. B. SUH, AND HIROSHI NIKAIDO*

Department of Molecular and Cell Biology, University of California, Berkeley, California 94720-3206

Received 21 April 1994/Accepted 5 December 1994

Accumulation of tetracycline in *Escherichia coli* was studied to determine its permeation pathway and to provide a basis for understanding efflux-mediated resistance. Passage of tetracycline across the outer membrane appeared to occur preferentially via the porin OmpF, with tetracycline in its magnesium-bound form. Rapid efflux of magnesium-chelated tetracycline from the periplasm was observed. In *E. coli* cells that do not contain exogenous tetracycline resistance genes, the steady-state level of tetracycline accumulation was decreased when porins were absent or when the fraction of Mg^{2+}-chelated tetracycline was small. This is best explained by assuming the presence of a low-level endogenous active efflux system that bypasses the outer membrane barrier. When influx of tetracycline is slowed, this efflux is able to reduce the accumulation of tetracycline in the cytoplasm. In contrast, we found no evidence of a special outer membrane bypass mechanism for high-level efflux via the Tet protein, which is an inner membrane efflux pump coded for by exogenous *tetA* genes. Fractionation and equilibrium density gradient centrifugation experiments showed that the Tet protein is not localized to regions of inner and outer membrane adhesion. Furthermore, a high concentration of tetracycline was found in the compartment that rapidly equilibrated with the medium, most probably the periplasm, of Tet-containing *E. coli* cells, and the level of tetracycline accumulation in Tet-containing cells was not diminished by the mutational loss of the OmpF porin. These results suggest that the Tet protein, in contrast to the endogenous efflux system(s), pumps magnesium-chelated tetracycline into the periplasm. A quantitative model of tetracycline fluxes in *E. coli* cells of various types is presented.

Active efflux of tetracycline (TC) is a resistance mechanism found in both gram-negative and gram-positive bacteria (5, 18). In the gram-negative bacterium *Escherichia coli*, efflux resistance genes have been identified on both plasmids and transposons (the *tet* genes) (27) and on the chromosome (the genes activated by the *marRAB* regulatory system [6, 11]). The TC resistance gene *tetA* (class B) in transposon Tn*10* (and other homologous resistance genes such as the *tetA* [class C] gene present in pBR322) codes for an integral inner membrane (IM) protein, Tet, which contains 12 transmembrane helices and belongs to a family of bacterial and eukaryotic transporters, the major facilitator family (5, 9, 18). The Tet protein binds TC in the cytoplasm and pumps it, possibly into the periplasm, in exchange for a proton, a process that is driven by the proton motive force across the IM (52).

Although TC can diffuse readily through the IM bilayer (2, 35), the lipid bilayer of the outer membrane (OM) is relatively impermeable to lipophilic solutes (38) such as TC, and TC is thought to cross the OM mainly via the porin OmpF (5). In mutants with decreased OmpF expression, there is an increase in the TC MIC (7, 25, 40). This observation was surprising for the following reason. If TC both enters and exits the cell through OmpF, one would expect that decreased OmpF levels should affect both the influx and efflux of TC equally and that the steady-state level of TC inside the cell would remain unchanged. In addition, it is not clear how pumping of TC into the periplasm by Tet leads to high levels of resistance, since TC should easily be able to reenter the cytoplasm by spontaneous diffusion.

* Corresponding author. Mailing address: Department of Molecular and Cell Biology, 229 Stanley Hall, University of California, Berkeley, CA 94720-3206. Phone: (510) 642-2027. Fax: (510) 643-9290.

In this investigation, we studied the permeation of TC under a variety of conditions. Our results are consistent with the notion that TC crosses the OM via the porin OmpF as Mg^{2+}-chelated TC ($TCMg^{+}$), whereas in porin-deficient cells it crosses the OM through its bilayer domains as uncharged TC (TCH). A low-level endogenous efflux system(s) that pumps TC directly into the medium appears to operate in wild-type cells; in contrast, the Tet protein pumps TC into the periplasm.

MATERIALS AND METHODS

Strains and media. The strains used in this study are listed in Table 1. HN819 was made by removing transposon Tn*10* from HN705 (48) as previously described (23). Cultures were inoculated from single colonies or, for OM mutants, from frozen stocks into Luria-Bertani broth (28). For growth in minimal medium, overnight cultures grown in Luria-Bertani broth were resuspended and diluted in medium 63 (M63) (28) containing 0.2% glucose, 0.1% Casamino Acids, 20 μg of the required supplements per ml, and 1 mM $MgSO_4$. All cultures were grown at 37°C with aeration by shaking.

Chemicals. [7-^{3}H]TC (0.80 to 0.89 Ci/mmol) was obtained from New England Nuclear Corp. as a powder. Portions were dissolved each week in 50% methanol and stored at −20°C as described in reference 26. TC hydrochloride and carbonyl cyanide *m*-chlorophenylhydrazone (CCCP) were obtained from Sigma Chemical Co.

TC accumulation measurement by the filtration method. Uptake experiments were performed essentially as described in reference 27. All such experiments were repeated at least twice, to make certain that the results were reproducible. Cells grown in M63 to the mid-exponential phase were harvested at room temperature, washed, and resuspended to 1.5 mg of protein ml^{-1} in prewarmed assay buffer. Assay buffer contained 50 mM K-phosphate (pH 7.0, unless specified otherwise), 0.2% glucose, 1 mM $MgSO_4$ (unless specified otherwise), plus any required nutrients. Portions of 1 ml each were removed and preincubated for 5 to 10 min at 37°C with shaking. [^{3}H]TC was then added to a final concentration of 5 μM. At time points thereafter, 50-μl portions were removed, diluted in 1 ml of wash buffer (containing 0.1 M K-phosphate [pH 7.0 or as specified] and 0.1 M LiCl), and filtered through a 0.45-μm-pore-size GN-6 Metricel filter (Gelman Sciences) on a vacuum filter manifold (Hoefer Scientific Instruments). The filter was washed rapidly twice with 4-ml portions of wash buffer and dried, and the radioactivity was determined in a Beckman LS 7000 liquid scintillation counter by using Ecolume (ICN Biomedicals) scintillation cocktail. In all cases, counts

TABLE 1. *E. coli* strains used in this study

Strain	Relevant phenotype (genotype)	Reference or source
CM6	$OmpF^+$ $OmpC^-$ (B/r *tonA mal*)	3
CM7	$OmpF^-$ $OmpC^-$ (B/r *tonA mal kmt-7*)	3
JF701	$OmpF^+$ $OmpC^-$ $PhoE^{repressed}$ (K-12 *ompC264 aroA ilv metB his purE cyc-1 xyl lacZ rpsL tsx*)	33
JF694	$OmpF^-$ $OmpC^-$ $PhoE^{constitutive}$ (as in JF701 but also *ompF254 nmpA1*)	34
JM101	$OmpF^+$ $OmpC^+$ (K-12 (*lac-pro*) *thi supE*/F′ *proAB*$^+$ *lacI*^{q} *lacZ* M15)	
HN819	$OmpF^-$ $OmpC^-$ (as in JM101 but also *ompC178 ompF*::Tn*5*)	This study
D1-1	K-12/R222[a]	S. B. Levy

[a] This plasmid codes for a class B TetA protein.

from label binding to filters alone were subtracted from the measured values. Protein assays were done with bicinchoninic acid reagent (Pierce) with bovine serum albumin as the standard (45).

TC accumulation measurement by the centrifugation method. For measurements by the centrifugation method, the above-described procedure was followed with the following modifications (see reference 14). At various time points, 50-μl portions were removed and layered on top of 150 μl of silicon oil (70% fluid no. 550 and 30% fluid no. 510 [50 cP]; Dow Corning Corp.) in 0.4-ml long-style microcentrifuge tubes (USA/Scientific Plastics, Ocala, Fla.). The tubes were centrifuged for 2 min in a microcentrifuge to pellet the cells and then frozen in dry ice-ethanol. The tip of each tube, containing the cell pellet, was cut into a scintillation vial, and the pellet was resuspended in 0.3 ml of water. Scintillation cocktail was added, and the vial was counted in a scintillation counter as described above. Counts obtained from the label alone were subtracted from the measured values.

TC accumulation in spheroplasts. Spheroplasts were made as described by Witholt and coworkers (50). Mid-exponential-phase cells grown in M63 were harvested and resuspended to 5 mg of protein ml^{-1} in 2 ml of 200 mM 2-amino-2-hydroxymethyl-1,3-propanediol (Tris)-HCl (pH 8.0). Two milliliters of 1 M sucrose in 200 mM Tris-HCl (pH 8.0) was added, followed by disodium EDTA to a final concentration of 0.5 mM. Lysozyme (from egg white; Sigma) was added to 60 μg ml^{-1}, and the suspension was diluted with 4 ml of water. The cells were allowed to stand at room temperature for approximately 20 min, and samples were checked periodically under a microscope for spheroplast formation. When spheroplast formation was complete, $MgSO_4$ was added to 5 mM and the spheroplasts were diluted with 20 ml of a solution containing 50 mM K-phosphate (pH 7.0), 5 mM $MgSO_4$, 20 mM Li-lactate, and 20% sucrose. The spheroplasts were centrifuged at room temperature, resuspended in 0.25 ml of the same buffer solution (except that it contained 1 mM $MgSO_4$ and 40 μg of pancreatic DNase [Sigma] ml^{-1}), and then diluted to a 4-ml final volume in the same buffer without the enzyme. Uptake experiments were performed at 30°C by the filtration method, except that the assay buffer contained 20 mM Li-lactate instead of glucose and both the assay and wash buffers contained 20% sucrose.

MIC determination. MIC was determined by twofold serial dilution in liquid Luria-Bertani broth with an inoculum of 2.5×10^4 cells per ml.

Membrane fractionation. For membrane fractionation, we used a procedure based on that described by Jacoby and Young (16). Strain D1-1 was grown in 200 ml of M63 to the late-exponential phase. For induction of the Tet protein, TC was added to 2 μg/ml. Cells were harvested (4,000 × *g*, 4°C, 10 min), washed with precooled 10 mM *N*-2-hydroxyethylpiperazine-*N*′-2-ethanesulfonic acid (HEPES)-NaOH buffer (pH 7.2), and resuspended in 3 ml of the same buffer containing 0.1 mM phenylmethylsulfonyl fluoride. Cells were broken by two passes through a French pressure cell (12,000 lb/in^2, 4°C). Unbroken cells were removed by centrifugation for 5 min at 12,000 × *g*, and 1 ml of the supernatant was loaded on top of 12 ml of a 20 to 60% (wt/wt) sucrose gradient (made in 10 mM HEPES). This was then centrifuged for at least 48 h in a Beckman SW41 rotor (150,000 × *g*, 4°C). Fractions were collected from the bottom of the gradient, and the density of the fractions was determined by measuring the refractive index on a refractometer (Fisher Scientific). NADH oxidase was assayed as previously described (37), and Western blotting (immunoblotting) was done with antibody raised against the carboxy-terminal sequence of the Tet protein (51), kindly provided by A. Yamaguchi, with alkaline phosphatase-conjugated secondary antibodies (13).

Distribution of various ionic forms of TC. To understand the cellular accumulation of TC on a quantitative basis, we wanted to calculate the passive distribution of TC into compartments of metabolizing *E. coli* cells. For this purpose, we have to know the fractional distribution of TC into its various ionic forms. TC has three protonation sites and therefore can exist in any of eight possible ionic forms: $A^0B^+C^0$, $A^-B^+C^0$, $A^0B^+C^-$, $A^-B^0C^-$, $A^-B^0C^0$, $A^-B^+C^-$, $A^0B^0C^-$, and $A^0B^0C^0$. The relative abundance of each of these forms can be calculated in the absence of Mg^{2+}, because microscopic dissociation constants have been determined (41). However, we do not know the affinity of each of these forms for Mg^{2+}, and thus we used the following approximate method to calculate the fractions of various forms in the presence of Mg^{2+}.

(i) The fraction of $TCMg^+$ was calculated as follows. The protonation of TC was assessed by using a simplified scheme: around neutral pH, most of the strongly acidic group A is deprotonated and most of the fairly strong basic group B is protonated. Thus, we should be concerned only with the dissociation of the weak acid C, which has a macroscopic pK_a of 7.7. The forms protonated and unprotonated at C are represented as TCH^{+-} and TC^-, respectively.

(ii) Chelation of Mg^{2+} occurs only with TC^-, with a dissociation constant of 1.26×10^{-4} M (1).

(iii) Consequently, at any pH, $[H^+][TC^-]/[TCH^{+-}] = K_A$ ($K_A = 10^{-7.7}$ M), $[Mg^{2+}][TC^-]/[TCMg^+] = K_{Mg}$ ($K_{Mg} = 1.26 \times 10^{-4}$ M), and $[TC^{tot}] = [TC^-] + [TCH^{+-}] + [TCMg^+]$, where $[TC^{tot}]$ is the total concentration of TC. Solution of these equations gives $[TCMg^+] = [Mg^{2+}][TC^{tot}]K_A/(K_{Mg}[H^+] + K_AK_{Mg} + K_A[Mg^{2+}])$.

(iv) The total concentration of unchelated TC species was calculated by subtracting $[TCMg^+]$ from $[TC^{tot}]$, and then this was used to calculate the concentration of the uncharged form $A^0B^0C^0$ (which we designate TCH) with the microscopic dissociation constants given by Rigler et al. (41), that is, by assuming that the relative abundance of various unchelated species is not affected by the presence of Mg^{2+}.

Predicted equilibrium distribution of TC in cells lacking active efflux mechanisms. The basic postulates are as follows. (i) In wild-type, susceptible *E. coli* containing OmpF porin, $TCMg^+$ is the major species of TC that crosses the OM (as shown in Results) and it penetrates through the porin channel. The equilibrium distribution of $TCMg^+$ is dictated by the Donnan potential across the OM.

(ii) The Donnan potential has a value of 26 mV (interior negative) for cells cultured in moderate-ionic-strength medium (M63) and resuspended in 50 mM buffer (43). Under these conditions, the periplasmic concentration of univalent cations such as $TCMg^+$ or H^+ is 2.75 times higher than that in the medium, and the concentration of divalent cations such as Mg^{2+} is 7.56 times higher than that in the medium (43).

(iii) Distribution of TC across the IM occurs so that the concentrations of the uncharged species, $A^0B^0C^0$ (or TCH), are equal on both sides of the IM. This species is expected to correspond to 4.94, 9.43, and 8.6%, of the unchelated TC molecules at pHs 7.8, 6.5, and 7.0, respectively, on the basis of reported microscopic dissociation constants (41).

(iv) Cytoplasmic pH is 7.8 (17). We have not been able to find data on the concentration of free Mg^{2+} in bacterial cytoplasm; we believe that it is reasonably close to the value in the eukaryotic cytosol, i.e., between 0.7 and 1.35 mM (42), and used a value of 1 mM. Results of these calculations are listed in Table 2.

RESULTS

Accumulation of TC in $OmpF^+$ and $OmpF^-$ cells without the extrinsic *tet* determinant. We first examined the permeation of TC into *E. coli* cells lacking the Tet efflux pump. Accumulation of TC in the isogenic *E. coli* B/r strains CM6 ($OmpF^+$ $OmpC^-$) and CM7 ($OmpF^-$ $OmpC^-$) was examined (Fig. 1). There was progressive accumulation of TC in the cells of both strains. Since proteins make up about 50% of the cell dry weight (30) and the cell volume is around 3 μl/mg of dry weight (29), the final accumulation level in CM6 (460 pmol/mg of protein) corresponds to about 75 μM, a concentration substantially higher than the external level of 5 μM. Although some of this is caused by binding to ribosomes (see Discussion), much is due to passive distribution of various ionic forms of TC across the membranes (35). Thus, $TCMg^+$ becomes concentrated in the periplasm following the Donnan potential (interior negative) across the OM and TC is further concentrated in the cytoplasm as it equilibrates across the IM so that the concentrations of the uncharged, IM-permeating species, TCH, become equal on both sides of the membrane. Because more TC exists in the dissociated form, TC^-, in the higher-pH environment of the cytoplasm (35), this passive equilibration produces a higher total concentration of TC in the cytoplasm (Table 2, experiment 1). The addition of a proton conductor such as CCCP abolishes ΔpH across the IM, and this accumulation in the cytoplasm consequently disappears (Fig. 1).

CM7 had approximately half of the steady-state uptake level of CM6 (Fig. 1). Consistent with the accumulation data, the

TABLE 2. Predicted equilibrium distribution of TC in *E. coli* cells[a]

Expt no., condition, and fraction tested	pH	Predicted concn (μM) of:				
		Mg^{2+}	TC^{tot}	$TCMg^{+}$	$TC^{tot} - TCMg^{+}$	TCH
1, 1 mM Mg^{2+}						
Medium	7.0	1,000	5.0	**2.85**	2.15	*0.185*
Periplasm	6.56	7,560	9.8	**7.83**	1.97	*0.185*
Cytoplasm	7.8	1,000	20.0	16.31	3.68	0.185
2, pH 6.0						
Medium	6.0	1,000	5.0	0.67	4.33	0.415
Periplasm	5.56	7,560	6.1	1.85	4.27	0.397
Cytoplasm	7.8	1,000	44.0	35.85	8.10	0.397
3, pH 7.8						
Medium	7.8	1,000	5.0	4.08	0.92	0.045
Periplasm	7.36	7,560	11.8	11.22	0.58	0.042
Cytoplasm	7.8	1,000	4.7	3.79	0.86	0.042
4, 0.03 mM Mg^{2+}						
Medium	7.0	30	5.0	0.19	4.81	0.413
Periplasm	6.56	227	4.8	0.52	4.31	0.404
Cytoplasm	7.8	1,000	44.2	36.02	8.14	0.404

[a] Calculations that led to the model described here are described in Materials and Methods. Note that under the conditions of experiment 1, the distribution between the medium and the periplasm is identical regardless of whether it is driven by the 2.75-fold-higher accumulation of $TCMg^{+}$ in the periplasm (boldface values) or by the equal distribution of the uncharged species across the membrane (italic values).

MIC of TC for CM6 was 1 μg/ml whereas that for CM7 was 8 μg/ml. The difference between these two strains is due solely to the OM, since spheroplasts of both strains showed identical uptake patterns (data not shown). Accumulation patterns similar to those of CM6 and CM7 were also seen for independently derived isogenic K-12 strains JM101 ($OmpF^{+}$ $OmpC^{+}$) and HN819 ($OmpF^{-}$ $OmpC^{-}$) (data not shown).

Low-level efflux of TC and, more noticeably, minocycline has been reported in wild-type cells (24). The presence of an endogenous active efflux system could explain the lower uptake in CM7 and other $OmpF^{-}$ strains. TC obviously penetrates through the OM of porin-deficient strains more slowly, but this factor alone would only delay attainment of a steady-state level, which should eventually become equivalent to that of the wild type. Slower influx in the presence of an endogenous active efflux, however, would allow the efflux system to lower the internal TC concentration more effectively, resulting in a lower steady-state concentration. Note that this requires that the efflux process bypass the OM barrier, because otherwise steady-state levels would again become identical in both $OmpF^{+}$ and $OmpF^{-}$ strains. This hypothesis can also explain the lack of CCCP effect in CM7 (Fig. 1). Thus, in CM7 the slower drug influx across the OM allows the endogenous active efflux system to reduce the cytoplasmic concentration of TC. Addition of CCCP inhibits this efflux, but it also inhibits influx of TC into the cytoplasm because of dissipation of the ΔpH across the IM, and therefore the net result is little to no change in the overall TC accumulation level.

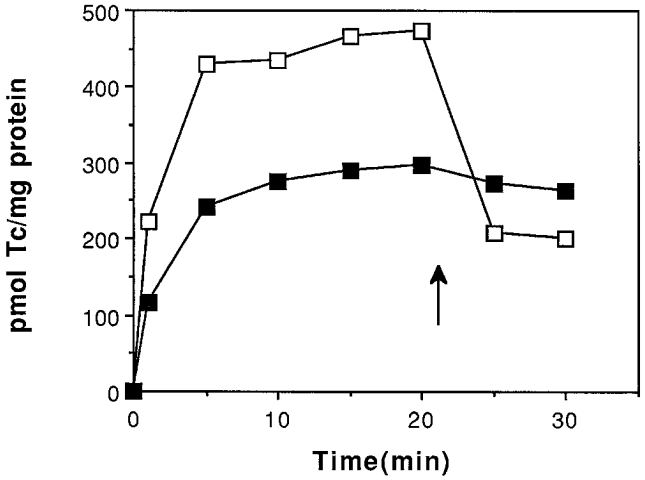

FIG. 1. TC accumulation by strains CM6 (□) and CM7 (■). Accumulation was measured by the filtration method in assay buffer containing 5 μM [^{3}H]TC and 1 mM Mg^{2+}. The arrow indicates addition of 100 μM CCCP.

Several more lines of data are consistent with the active-efflux hypothesis. For example, lowering the pH of the external medium increased very significantly the steady-state accumulation of TC in CM7 (Fig. 2A). A lower pH is expected to increase the fraction of forms protonated at the acidic group with a pK_a of 7.7, including TCH (Table 2, experiment 2, medium). In porin-deficient strains such as CM7, TC most likely enters cells by diffusing through the OM lipid bilayer region in the uncharged, protonated form, TCH (35). The increased concentration of TCH in the medium then produces a higher rate of uptake across the OM bilayer, and consequently the steady-state accumulation level is increased (Fig. 2A). Note that at pH 6, there is sufficient uptake into CM7 to allow for concentration of TC in the cytoplasm and subsequent loss of accumulation upon CCCP addition. In contrast, with CM6 there was less accumulation of TC at pH 6 than at pH 7 (Fig. 2B). TC is likely to cross the OM of CM6 through the OmpF porin channel mainly as $TCMg^{+}$ (see also below), and the drastic decrease in $TCMg^{+}$ at pH 6 (Table 2, experiment 2, medium) presumably slows down the influx significantly. Thus, the contribution of active efflux becomes more significant and the cytoplasmic level never reaches the high level expected for true equilibrium across the IM. At pH 7.8, the accumulation level in CM7 decreased (Fig. 2A), presumably because the fraction of the species that penetrates across the OM, TCH, became very small in the medium (Table 2, experiment 3, medium), and this slowed down the rate of entry of TCH. Decreased uptake in CM6 at pH 7.8 (Fig. 2B) was most probably due to the lower concentration of TCH in the periplasm, which produced less accumulation in the cytoplasm (Table 2, experiment 3, cytoplasm).

That TC normally crosses the OmpF porin channel as $TCMg^{+}$ is supported by comparison of isogenic strains JF701 ($OmpF^{+}$ $OmpC^{-}$ $PhoE^{repressed}$) and JF694 ($OmpF^{-}$ $OmpC^{-}$ $PhoE^{constitutive}$) (Fig. 3). JF694 lacks OmpF but expresses PhoE, a porin that has a pore size comparable to that of OmpF but is anion selective (36). The lower TC accumulation and lack of CCCP response in this strain show that if TC cannot cross the OM rapidly as $TCMg^{+}$, the steady-state level becomes lowered significantly because of the endogenous efflux process.

$TCMg^{+}$ can rapidly exit across the OM. Two procedures were used in this study to measure TC accumulation (see Materials and Methods): one based on filtration and one based on centrifugation. The main difference between these two methods is that the filtration method requires dilution and wash steps, which are not necessary in the centrifugation method. When we measured TC uptake by CM6 cells in 1 mM Mg^{2+} by the two methods, we obtained an unexpected result: the accumulation level determined by centrifugation (Fig. 4B,

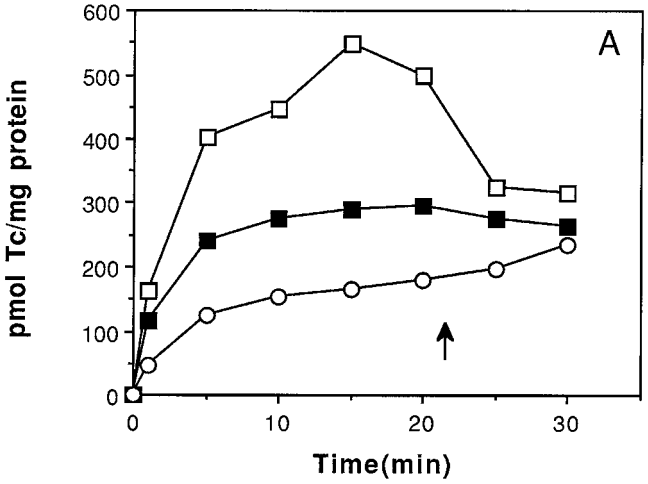

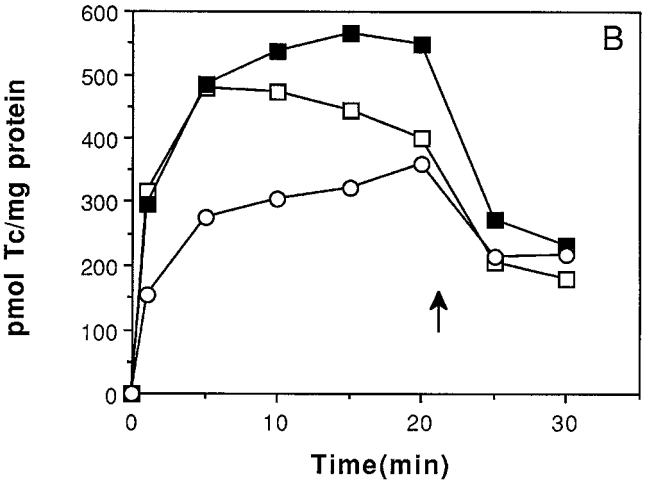

FIG. 2. Effect of pH on TC accumulation by strains CM7 (A) and CM6 (B). Accumulation was measured by the filtration method in assay buffer containing 5 μM [^{3}H]TC and 1 mM Mg^{2+} at pHs 6.0 (□), 7.0 (■), and 7.8 (○). The arrow indicates addition of 100 μM CCCP.

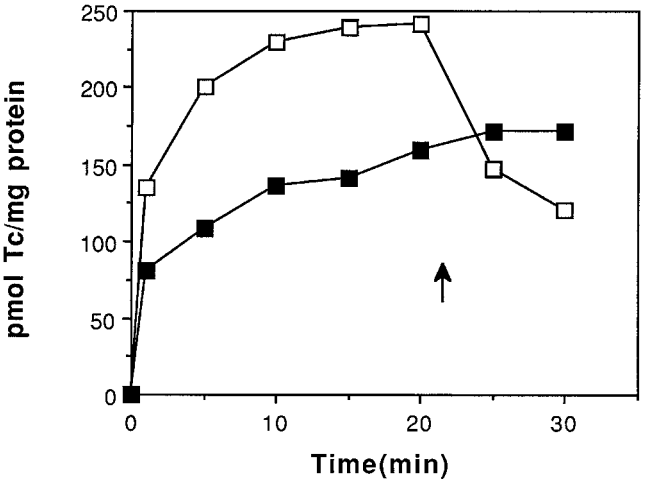

FIG. 3. TC accumulation by strains JF701 (□) and JF694 (■). Accumulation was measured by the filtration method in assay buffer containing 4 μM [^{3}H]TC and 1 mM Mg^{2+}. The arrow indicates addition of 100 μM CCCP.

closed squares) was much higher than that determined by filtration (Fig. 4A, closed squares). This suggests that in the filtration method, the dilution and wash steps allow efflux of TC from the periplasm into the wash buffer. As shown above, the major route of passage across the OM for TC is via OmpF in the $TCMg^+$ form. At a 1 mM Mg^{2+} concentration, nearly 60% of the TC in the periplasm is in the chelated form (Table 2, experiment 1), and thus TC is expected to diffuse out rapidly during washing. The centrifugation method eliminates the dilution and wash steps. It therefore does not allow significant leakage of TC from the periplasm, and it measures the sum of cytoplasmic and periplasmic TC.

This hypothesis was supported by carrying out the dilution and washing steps at 0°C. Low temperature inhibits diffusion through lipid bilayers (31) but does not affect diffusion through porins (33). Thus, diffusion of TC through the IM is prevented but diffusion through the OM is allowed. Under these conditions, significant differences in accumulated levels were still found between the centrifugation and filtration methods when 1 mM Mg^{2+} was present (data not shown). This indicates that leakage during washing indeed occurs through the OM, and not from the cytoplasm through the IM.

Additional support for this interpretation comes from a comparison of the two methods at 0.03 mM Mg^{2+}. At this concentration of Mg^{2+}, only 10% of TC in the periplasm is expected to exist in the chelated form (Table 2, experiment 4, periplasm), and leakage of TC during washing is expected to be slow. Indeed, the filtration and centrifugation methods showed nearly identical accumulation levels (Fig. 4, open squares).

Calculations based on equilibrium distribution predicted greater accumulation of TC in the cytoplasm at the lower Mg^{2+} concentration (compare experiments 1 and 4 in Table 2), but the total accumulation levels obtained by centrifugation were about the same regardless of the concentration of Mg^{2+} (Fig. 4B). This provides more support for the endogenous-efflux hypothesis. Thus, the influx of TC across the OM occurs more slowly at 0.03 mM Mg^{2+}, owing to the scarcity of $TCMg^+$ species in the medium (Table 2, experiment 4). Under these conditions, the endogenous active-efflux system becomes more effective, preventing increases in the steady-state TC level in the cytoplasm.

Tet protein pumps $TCMg^+$ into the periplasm. We next examined efflux of TC in strains containing the extrinsic *tet* efflux determinant. The Tet protein has been shown to bind and pump out $TCMg^+$, possibly into the periplasm (53). Comparison of the filtration and centrifugation methods as described above showed that we can measure, at least approximately, TC in the periplasm, and we therefore attempted such quantitation in cells expressing the Tet protein. Accumulation of TC in CM6 cells transformed with plasmid pBR322, which carries a constitutively expressed copy of the *tetA* (class C) gene, was measured by both methods. As shown in Fig. 5, uptake measured by the centrifugation method was approximately 10-fold higher than uptake measured by the filtration method, indicating that a large amount of TC is actually located in the periplasm of these cells and that the Tet protein must pump TC into the periplasm and not directly out of the cells.

Results obtained with CM7 containing pBR322 are also consistent with this model. These cells accumulated a higher

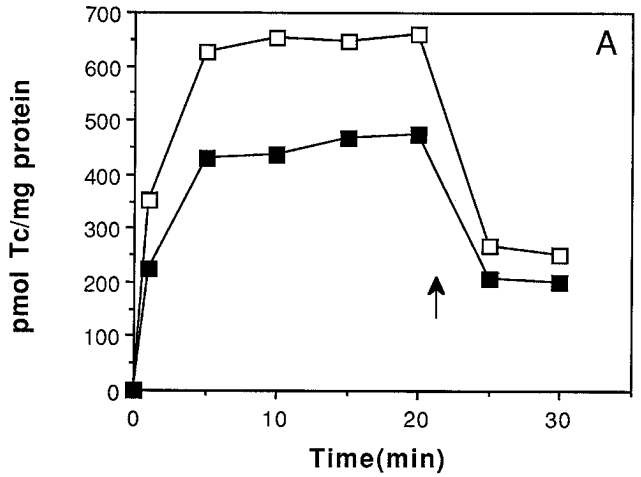

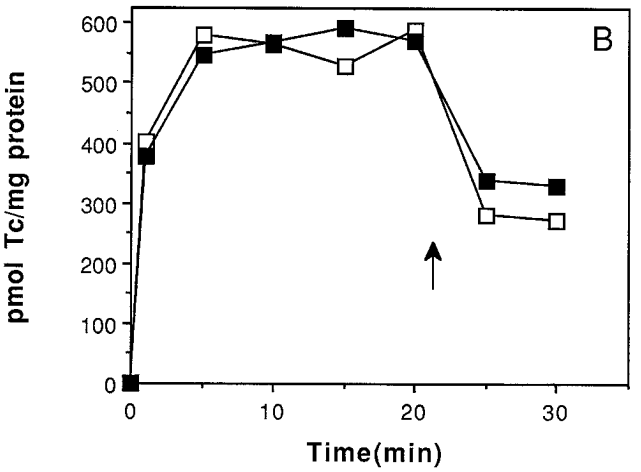

FIG. 4. Accumulation of TC by strain CM6 measured by the filtration (A) and centrifugation (B) methods. Cells were incubated in assay buffer containing 5 μM [^{3}H]TC and either 0.03 (□) or 1 (■) mM Mg^{2+}. The arrows indicate addition of 100 μM CCCP.

level of TC than did CM6/pBR322 cells, as measured by the filtration method (Fig. 6). If the Tet-mediated efflux bypassed the OM, CM7/pBR322 cells would show a much lower TC accumulation level, since influx is much slower in this strain. In contrast, if Tet pumps $TCMg^+$ into the periplasm, rather than directly into the medium, a steady state will be achieved when the periplasmic concentration of TC reaches equilibrium with the external concentration of TC. This steady state should be dictated only by the pumping of TC into the periplasm by the Tet protein and should not be affected by the permeability of the OM. In other words, in $OmpF^-$ strains, influx and efflux across the OM will be equally slowed and the steady state-level of TC will not change. In support of this, the MIC for both CM6/pBR322 and CM7/pBR322 was 128 μg ml^{-1}, in striking contrast to the eightfold difference between the MICs of the plasmid-free parent strains. The higher accumulation level actually observed for CM7/pBR322 than for CM6/pBR322 (Fig. 6) undoubtedly reflects the fact that the periplasmic TC does not diffuse out readily during washing when porins are absent. This again reinforces the conclusion that, in wild-type strains,

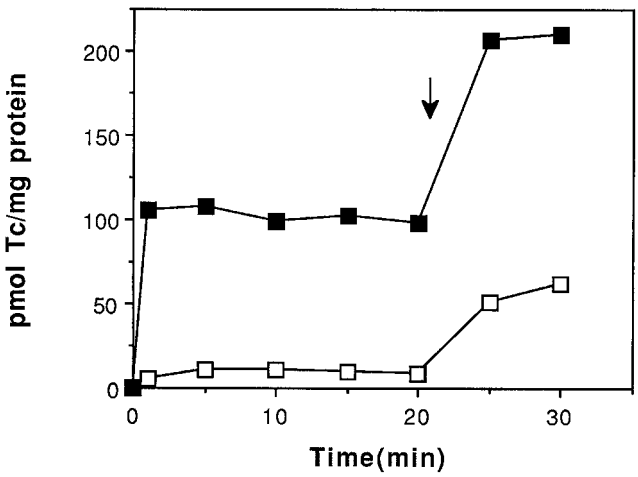

FIG. 5. TC accumulation by CM6/pBR322. Accumulation was measured by the filtration (□) or centrifugation (■) method in assay buffer containing 5 μM [^{3}H]TC and 1 mM Mg^{2+}. The arrow indicates addition of 100 μM CCCP.

$TCMg^+$ rapidly diffuses through the OmpF porin channel, both inwards and outwards.

Tet protein is not located at regions of membrane fusion. Finally, we would expect that if the Tet protein pumped TC directly into the medium, rather than into the periplasm, the Tet protein would be associated with an OM channel, and probably with a linker protein to connect the IM pump with the OM channel, as has been observed in several systems (8, 10, 21, 22, 32). We looked, therefore, to see if the Tet protein might be inserted at regions of IM and OM adhesion, known as Bayer junctions (4). D1-1 cells, which carry the Tn*10 tetA* (class B) gene on an R plasmid, were induced for expression of the Tet protein, and the membranes were disrupted by two passes through a French pressure cell. The cells were then subjected to equilibrium centrifugation through a continuous sucrose gradient. It has been demonstrated that in such a gradient the OM migrates to the denser bottom fractions because of the presence of lipopolysaccharide and that the IM forms bands towards the top. In addition, there is a population of mem-

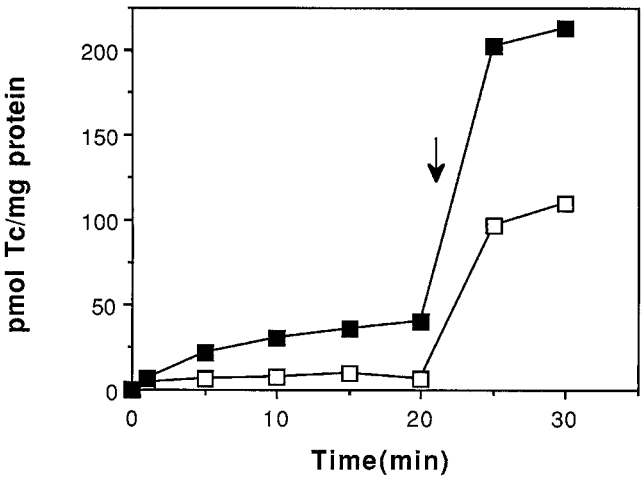

FIG. 6. Comparison of TC accumulation by strains CM6/pBR322 (□) and CM7/pBR322 (■). Accumulation was measured by the filtration method in assay buffer containing 5 μM [^{3}H]TC and 1 mM Mg^{2+}. The arrow indicates addition of 100 μM CCCP.

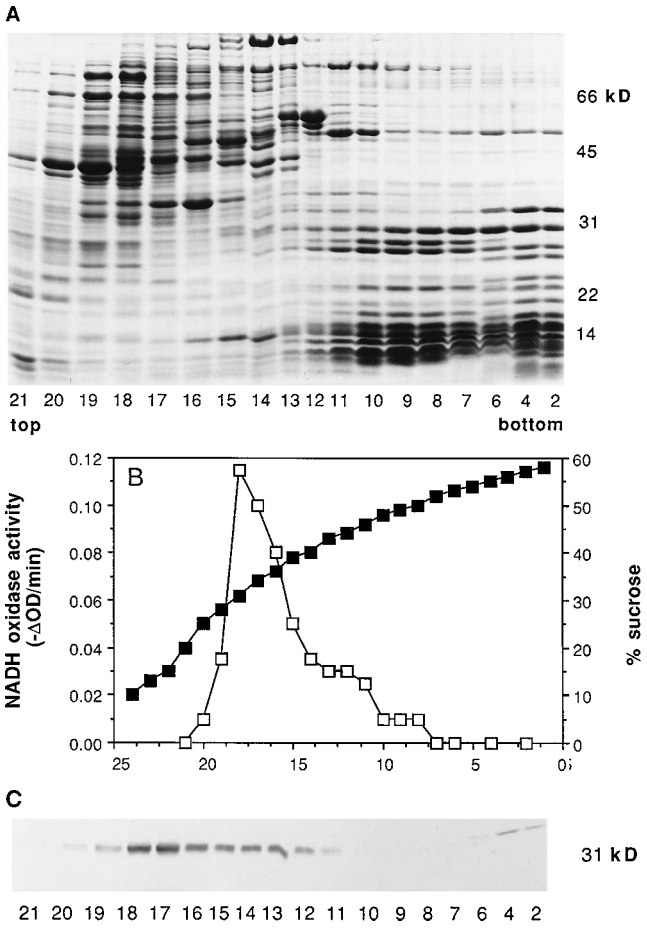

FIG. 7. (A) Distribution of membrane proteins of strain D1-1 following disruption by French press and equilibrium density gradient centrifugation. Fractions (20 drops) were collected and concentrated, and 20 μg of protein per lane was loaded onto a sodium dodecyl sulfate–11% polyacrylamide gel for slab gel electrophoresis (47). Proteins were visualized by staining with Coomassie brilliant blue. kD, kilodaltons. (B) Localization of IM proteins by NADH oxidase activity. NADH oxidase activity of the gradient fractions shown in panel A was measured as previously described (37). OD, optical density. (C) Immunoblot visualization of the Tet protein. Following electrophoresis, proteins were transferred onto a nitrocellulose membrane and probed for the Tet protein with an anti-Tet antibody. Antibody binding was visualized with alkaline phosphatase-conjugated anti-rabbit immunoglobulin G.

branes that migrate to intermediate-density regions which have been shown to contain fragments of attached IM and OM (4, 15, 16).

The protein profile from induced D1-1 cells after gradient centrifugation (Fig. 7A) shows a clear segregation of proteins into different portions of the gradient. Localization of IM proteins was determined by measuring NADH oxidase activity, which is due to the electron transport complex located in the IM. Figure 7B shows that, as expected, the IM is confined to the lower-density fractions, with a small portion extending into the middle of the gradient. Finally, localization of the Tet protein was monitored by using an antibody to the Tet protein in Western blots (immunoblots) of the gradient fractions. The antibody binding (Fig. 7C) colocalizes with the NADH oxidase activity, indicating an IM location for the Tet protein. Identical results were obtained by using [^{35}S]Met-labeled Tet protein (data not shown). We therefore found no evidence of insertion of the Tet protein at membrane fusion sites.

DISCUSSION

Qualitative analysis of results. As has been observed in many earlier studies (for references, see reference 35), we found that TC is accumulated in the cytoplasm of wild-type *E. coli* cells. Passive accumulation caused by the Donnan potential across the OM and ΔpH across the IM predict that the cytoplasmic concentration of TC will reach 20 μM when the external TC concentration is 5 μM, under our assay conditions (Table 2). The experimentally observed total TC concentration in CM6 cells was around 75 μM (see Results). However, as there are 20,000 ribosomes per cell and 1 mg of dry weight corresponds to 10^9 cells (30), up to 30% of the accumulated TC is likely to be bound to the ribosomes. Thus, the total cellular concentration of free TC observed was about 40 to 50 μM, which was not too far from what was predicted (20 μM), given the margin of error present in many of the assumptions. This result suggests that the accumulation of TC in wild-type *E. coli*, at pH 7.0 and in the presence of 1 mM Mg^{2+}, can be explained largely without assuming the presence of active efflux.

Examination of TC accumulation in various strains and under various conditions nevertheless suggested the presence of an endogenous efflux pump, even in susceptible *E. coli* strains. Our results suggest the following model. (i) TC crosses the OM of the wild-type strain rapidly through the OmpF channel, mainly as $TCMg^+$. This is supported by a comparison of $OmpF^+$ and $OmpF^-$ strains (Fig. 1) and $OmpF^+$ and $OmpF^-$ $PhoE^+$ strains (Fig. 3). It is also supported by accumulation experiments at pH 6.0 (Fig. 2B) and at 0.03 mM Mg^{2+} (Fig. 4; see explanation in Results). Furthermore, the known dimensions of the TC-metal complex (16a) suggest that $TCMg^+$ can go through the OmpF porin channel. (ii) In porin-deficient strains, TC slowly crosses the OM through the bilayer region, primarily as TCH (Fig. 1 and 2A). (iii) Wild-type *E. coli* appears to actively pump TC out of the cytoplasm by a mechanism that bypasses the periplasm and the OM barrier. This efflux activity reduces the steady-state accumulation level of TC whenever the influx is slow, for example, in porin-deficient strains (Fig. 1). The effect of the efflux activity also begins to show, even in $OmpF^+$ strains, whenever the fraction of $TCMg^+$ becomes small, for example, at pH 6 (Fig. 2B) or in the presence of lower concentrations of Mg^{2+} (Fig. 4). The concept of a balance between influx and endogenous efflux was presented more than a decade ago by McMurry et al. (24). (iv) In resistant strains possessing the extrinsic *tet* determinant, TC is pumped efficiently from the cytoplasm to the periplasm (Fig. 5). The Tet pump does not bypass the OM barrier, and therefore the permeability of the OM does not affect the steady-state level of accumulation, as indicated by the identical TC MICs observed in $OmpF^+$ and $OmpF^-$ strains containing pBR322 (see Results). (v) Under certain conditions, for example, in the presence of 1 mM Mg^{2+} and in the presence of the Tet pump, much $TCMg^+$ exists in the periplasm and appears to rapidly diffuse out of the cell via the OmpF porin during the dilution-washing process of the filtration assay (Fig. 5).

An alternative hypothesis could be invoked to explain the lower steady-state accumulation levels in porin-deficient strains such as CM7 and HN819. In this hypothesis, it is assumed that the steady-state levels reflect true equilibration across the membranes. Since TC crosses the OM of porin-deficient strains mostly as TCH (Results) and since neutral TCH would not respond to the Donnan potential, less accumulation of TC in the periplasm, and hence in whole cells, is thought to occur in $OmpF^-$ cells.

When the periplasmic concentration of TC was calculated on the basis of the dissociation behavior of TC, its affinity to Mg^{2+}, and the Donnan potential (see Materials and Methods), it was indeed shown that the total periplasmic concentration of TC in $OmpF^{+}$ cells would be higher than the concentration in the medium (Table 2, experiment 1). However, calculation showed that equilibration of uncharged TCH across the OM also produced a higher total concentration of TC in the periplasm. This is because the Donnan potential increases the periplasmic Mg^{2+} concentration, which sequesters away much of the periplasmic TC as $TCMg^{+}$ regardless of the route of entry of TC into the periplasm. This alternative hypothesis therefore cannot explain the observed differences in behavior between CM6 and CM7 (Fig. 1).

Mathematical modeling of TC penetration. (i) Construction of a model. For quantitative analysis of our experimental data, a theoretical model of TC entry and efflux was constructed. Diffusion of TC into *E. coli* cells can be modeled quantitatively as follows.

(a) Diffusion across the OM. Fick's first law of diffusion specifies that the permeation rate is equal to the product of the permeability coefficient, P_o (in centimeters per second), the area of the OM, A_o (in square centimeters per milligram), and the difference in TC concentrations across the OM (in nanomoles per cubic centimeter). The Donnan potential across the membrane, however, affects the equilibrium, which is attained when the total TC concentration in the periplasm, C_p, becomes about twice that of the external TC concentration, C_o, under our standard conditions (Table 2, experiment 1). Thus, the periplasmic TC behaves as though its effective concentration were $C_p/2$ and the rate of TC permeation (in nanomoles per milligram per second) will be proportional to $C_o - (C_p/2)$ as follows:

$$P_o \cdot A_o \cdot [C_o - (C_p/2)] \quad (1)$$

(b) Passive diffusion across the IM. Passive diffusion across the IM also follows Fick's first law of diffusion. The permeability coefficient of the IM is P_i, the area of the IM is A_i (in square centimeters per milligram), and the cytoplasmic TC concentration is C_c (in nanomoles per cubic centimeter). Again, the cytosolic TC behaves as though its effective concentration were $C_c/2$, resulting in an equilibrium distribution with C_c about twice as high as C_p (Table 2, experiment 1). The rate of TC permeation is

$$P_i \cdot A_i \cdot [C_p - (C_c/2)] \quad (2)$$

(c) The drug in the cytoplasm is pumped out by an active-efflux pump. The rate at which the drug is pumped out of the cytoplasm follows the Michaelis-Menten equation:

$$(C_c \cdot V_{\max})/(C_c + K_m) \quad (3)$$

where $V_{\max}$ and K_m are the usual parameters of the catalyzed process.

The entry and exit of TC are described by a set of differential equations combining the rates defined above. We have designated the cytoplasmic and periplasmic volumes V_c and V_p (in cubic centimeters per milligram), respectively, and dC/dt is the variation of the specified TC concentration with respect to time t. If efflux occurs directly into the medium, then

$$dC_p/dt = (1/V_p \{P_o \cdot A_o \cdot [C_o - (C_p/2)] - P_i \cdot A_i \cdot [C_p - (C_c/2)]\} \quad (4)$$

$$dC_c/dt = (1/V_c) \{P_i \cdot A_i \cdot [C_p - (C_c/2)] - [(V_{\max} \cdot C_c/(K_m + C_c)]\} \quad (5)$$

If efflux occurs into the periplasm, then

$$dC_p/dt = (1/Vp) \{P_o \cdot A_o \cdot [C_o - (C_p/2)] - P_i \cdot A_i \cdot \{C_p - (C_c/2)] + [(V_{\max} \cdot C_c)/(K_m + C_c)] \quad (6)$$

(ii) Numerical values of the parameters. The values of the following parameters are known with reasonable precision from the references cited. A_o is 132 cm^2/mg of dry weight (44); V_c is 0.0024 cm^3/mg of dry weight, and V_p is 0.0006 cm^3/mg of dry weight because the total cell volume is about 0.003 cm^3/mg (29) and the periplasm occupies about 20% of the total cell volume (47). A_i is estimated as 105 cm^2/mg of dry weight from the dimensions of the cell (44) and from the fraction occupied by the periplasmic space.

P_i was estimated as follows. The apparent partition coefficient of TC in octanol-water at pH 7.4 is reported to be 0.034 (12). In general, the partition coefficients in oil-water systems are at least 10-fold lower than those in an octanol-water system (12), and this was also confirmed with TC in our laboratory (49). We therefore estimated that the apparent oil-water partition coefficient of TC is about 0.003. Since only 7% of TC exists in the uncharged form at this pH in the absence of Mg^{2+} (41), the true partition coefficient of the uncharged form, TCH, is 0.003/0.07 = 0.04. The permeability coefficient of lipophilic solutes through a typical membrane bilayer can be estimated from the relationship established by Collander (see reference 46), $P = 0.03\ K/(MW)^{1/2}$, where P, K, and MW are the permeability coefficient (in centimeters per second), the oil-water partition coefficient, and molecular weight, respectively. Thus, the permeability coefficient of TCH across the IM is predicted to be 6×10^{-5} cm s^{-1}. However, Collander's experiments were carried out at room temperature and our experiments were done at 37°C. From the temperature dependence of permeability coefficients of small solutes (46), we estimate that under our conditions the permeability coefficient of TCH at 37°C is around 1.8×10^{-4} cm s^{-1}. Since only 1.9% of the total periplasmic TC exists as TCH under our conditions (Table 2, experiment 1), this means that the permeability coefficient, P_i, expressed in terms of the total TC concentration, is $0.019 \times 1.8 \times 10^{-4}$, or about 3×10^{-6} cm s^{-1}.

(iii) Solution of differential equations. Either equations 4 and 5 or 6 and 5 were solved numerically with the fourth-order Runge-Kutta method by using the Mathcad Plus, version 5.0, program (Mathsoft, Cambridge, Mass.). As the initial condition, $C_p = C_c = 0$ (at $t = 0$) was used. We used a C_o value equal to the MIC for each strain, because under these conditions C_c is expected to attain a value at which ribosomes just become inhibited, a concentration determined previously to be around 10 μM (19).

(a) Porin-deficient *E. coli* not containing Tet protein. TC is likely to cross the bilayer domain of the OM of these cells as TCH. Our previous studies indicated that the permeability of the OM bilayer is lower, by a factor of up to 100, than the permeability of the IM bilayer (38). In view of the permeability coefficient of TCH across the IM, described above, we can expect a coefficient of $1.8 \times 10^{-4} \div 100 = 1.8 \times 10^{-6}$ cm s^{-1} for TCH across the OM. Since TCH is 3.7% of the total TC in the medium (Table 2, experiment 1), P_o, defined in terms of the total TC concentration, is $0.037 \times 1.8 \times 10^{-6} = 0.7 \times 10^{-7}$ cm s^{-1}. McMurry et al. (24) found that minocycline efflux by susceptible *E. coli* cells had a K_m higher than 100 μM, and so we assumed the *Km* to be 200 μM. We varied the one unknown parameter, $V_{\max}$, in the numerical integration of simultaneous equations 4 and 5. The results showed that at a $V_{\max}$ of 0.2 nmol mg^{-1} min^{-1}, CM7 cells in the presence of 8 μg of TC per ml (20 μM), which is equal to the MIC, were expected to

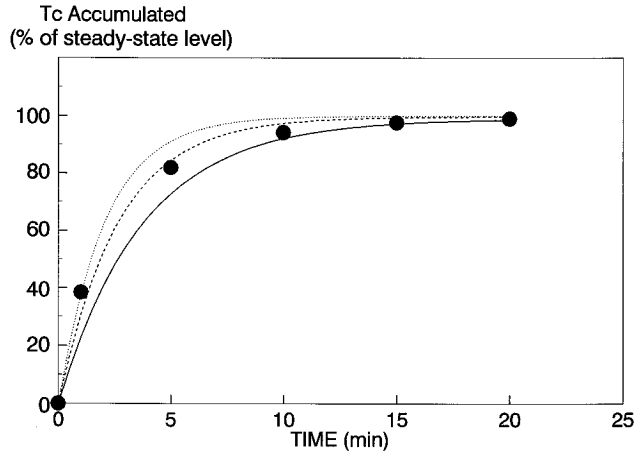

FIG. 8. Theoretically predicted progress curves and observed accumulation of TC in CM7. Progress curves of cytoplasmic TC concentration (C_c) were generated by assuming the presence of direct efflux pumps with V_{max} values of 0.1 (——), 0.2 (– – – –), and 0.25 (• • •) nmol mg^{-1} min. Other parameters are specified in the text, except that the external TC concentration, C_o, was set at 5 μM, our standard assay condition. Closed circles represent the observed kinetics of accumulation from Fig. 1. With the listed V_{max} values, it is predicted that the steady-state C_cs will be 15, 11, and 8 μM, respectively, when the C_o is 20 μM.

achieve a steady-state intracellular TC concentration of 11 μM, close to the anticipated growth-inhibitory concentration (19) of 10 μM. The predicted accumulation kinetics was also fairly close to the actual results (Fig. 8). At steady state, TC influx is limited by the OM barrier and this slow influx is effectively counterbalanced by the slow endogenous efflux directly into the medium, so that neither the periplasm nor the cytoplasm is in equilibrium with the TC in the medium (Fig. 9A).

(b) Porin-containing *E. coli* cells without Tet protein. In a wild-type strain, TC appears to cross the OM via OmpF rapidly as $TCMg^+$ (see above). In solving differential equations 4 and 5, we utilized V_{max} and K_m values that produced adequate simulations for porin-deficient cells, that is, 200 μM and 0.2 nmol mg^{-1} min^{-1}. One unknown parameter here is P_o. No reliable measurement of the diffusion rates of cationic solutes through the porin channel exists. Therefore, we solved the equations by using various values of P_o. The solutions indicated that if P_o is 10^{-5} cm s^{-1} at the external concentration of TC equal to the MIC (1 μg/ml or 2.5 μM), the cytoplasmic concentration will reach a steady-state level of 9 μM, close to the predicted inhibitory concentration of 10 μM. The model shows that at steady state, the efflux can lower the cytoplasmic concentration only a little from the equilibrium concentration of 10 μM, because the influx is relatively rapid (Fig. 9B). The periplasmic TC concentration is about 80% of the concentration expected at equilibrium. (The achievement of a steady state is predicted to be complete within 2 min, and our accumulation experiments, such as that described in Fig. 1, did not have sufficient time resolution to test whether the kinetics followed the predicted course). This permeability coefficient was in the range of those for many hydrophilic cephalosporins with sizes similar to that of TC (34). More importantly, the mathematical simulation predicted that 5- and 10-fold decreases in P_o would decrease the steady-state level by 20 and 35%, respectively. This fits the observation that lowering the pH of the medium to 6.0, which decreases the concentration of $TCMg^+$ about fourfold, results in observable decreases in the accumulation level (Fig. 2B). We note that assumed P_o values much higher than 10^{-5} cm s^{-1} do not produce this effect, although the predicted steady-state levels remain close to 9 μM.

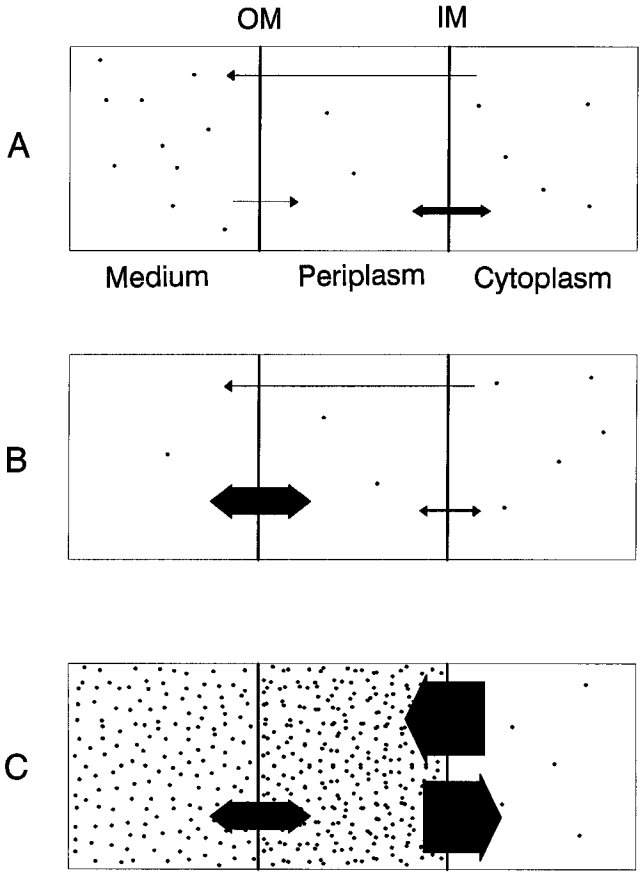

FIG. 9. Hypothetical models of TC fluxes in porin-deficient *E. coli* cells without the Tet protein (A), porin-containing cells without the Tet protein (B), and cells expressing the Tet protein (C). The models show the fluxes at steady state, when the external TC concentration is equal to the MIC. The density of dots corresponds roughly to the concentration predicted for each compartment, with the cytoplasm containing a level of TC just sufficient to inhibit protein synthesis. Single-headed arrows show nearly unidirectional fluxes. Double-headed arrows indicate near-equilibrium situations. Arrow thickness indicates, qualitatively, the rates of entry and exit. However, for double-headed arrows, the thickness does not indicate the actual net rates, which were close to zero. Rather, they indicate maximal possible rates in the presence of the steepest concentration gradient possible. This figure is intended to convey the notion that in porin-deficient cells the rate-limiting influx across the OM is balanced by the endogenous efflux, with the cytoplasm essentially in equilibrium with the periplasm (A); that in wild-type cells, both compartments are not far from equilibrium (B); and that in Tet-containing cells, a steady state occurs because the spontaneous influx of TC across the IM is balanced by its rapid active efflux across the IM (C).

(c) *E. coli* producing the Tet protein. Our results suggested that TC is pumped out into the periplasm. This can be modeled by using differential equations 6 and 5. Most of the parameters are known from the analyses described above. We used the experimentally determined K_m value of the Tet pump, 10 μM (27). The V_{max} value was varied as the unknown parameter. When the external TC concentration is equal to an MIC of 128 μg/ml or 300 μM, an assumed V_{max} of 20 nmol mg^{-1} min^{-1} produced the predicted steady-state cytoplasmic TC concentration of 9.3 μM. This value of V_{max} is not so far from the V_{max} experimentally determined with membrane vesicles from cells containing the Tn*10* class B *tet* determinant on plasmids, 5.2

nmol mg^{-1} min^{-1} (converted from the reported value of 2.6 nmol mg [protein]$^{-1}$ min^{-1}; reference 53). The discrepancy between these two values is not significant, since our system contained a class C, rather than a class B, *tet* determinant and since measurements of transport activity in subcellular systems rarely reveal the full rates found in intact cells. The modeling thus reveals that Tet-containing cells have very low cytoplasmic TC concentrations but their periplasmic TC concentration is very high, essentially in equilibrium with the external TC concentration (Fig. 9C), in full agreement with the results of Fig. 5.

In this analysis, we assumed that the difference between the accumulation levels in the centrifugation and filtration assays reflects largely the TC in the cytoplasm. An alternative interpretation is that it corresponds to TC adsorbed to the bacterial cell surface, which is washed away only in the filtration assay. The latter hypothesis is not supported by the data. For example, much of the TC found in CM7/pBR322 cells could not be removed by filtration and washing (Fig. 6 and the centrifugation assay result [not shown]), in contrast to the finding obtained with CM6/pBR322 cells (Fig. 5), and it is unreasonable to expect that adsorption to the cell surface was very different between isogenic strains. Further, the model predicts that the periplasmic TC in Tet-containing cells is in equilibrium with the TC in the medium. Thus, we can calculate that 1 mg of CM6/pBR322 cells contains an amount of TC that corresponds to $V_p \times C_p$, or $0.003 \times 10 = 0.03$ nmol in the periplasm. The observed difference between the two assay methods in Fig. 5 was 0.045 nmol mg (dry weight)$^{-1}$ (or 0.09 nmol mg [protein]$^{-1}$), which is not far from the predicted value. It is unlikely that such agreement would occur if the differences between the two assays were due to surface binding.

Direct efflux versus efflux into the periplasm. In this report, we have presented what we believe to be the first rigorous theoretical model of non-steady-state accumulation kinetics of TC. It is reassuring that conclusions from our qualitative model were fully confirmed by this mathematical model, although this does not necessarily mean that every parameter we used is correct. Nevertheless, the quantitative model allows us to understand certain features of the efflux-based resistance in precise terms. One important feature is the confirmation that OM permeability has essentially no influence when efflux occurs into the periplasm, as by the Tet system. Thus, the cytoplasmic TC concentration in Tet-containing cells is determined essentially by the balance between the spontaneous influx through IM and the efflux into the periplasm. The periplasmic concentration increases until it reaches the level that is in equilibrium with the external TC. This predicts that more lipophilic derivatives of TC, such as minocycline, would diffuse across the IM more rapidly and therefore be more effective against Tet-containing strains, and the prediction seems to have been borne out (25). Since the lipid bilayer of IM has high permeability even for TC, the efflux process has to be efficient to counterbalance this influx. Indeed, the estimated V_{max} for the Tet system was about 100 times higher than the V_{max} predicted for the endogenous system. More correctly, we can calculate, by using the CM7 model, how large a V_{max} value is needed for the same endogenous pump (with a presumed K_m of 200 μM) to produce an MIC of 8 μg/ml, if the pump exported TC into the periplasm. This modeling led to a value of 15 nmol mg^{-1} min^{-1}, showing that the pump needs $15/0.2 = 75$ times higher activity to produce the same level of resistance if the drug is pumped into the periplasm rather than directly into the medium. On the other hand, independence from OM permeability may give a certain advantage to Tet-type pumps, since they are usually encoded by plasmid genes and are expected to produce resistance in a variety of bacteria with different OMs.

Direct efflux into the medium, in contrast, produces resistance only when OM permeability is low, as in CM7. This is probably the reason why endogenous efflux pumps produce high-level TC resistance in *Pseudomonas aeruginosa*, with its low-permeability OM (20), but has little effect on the TC MIC in wild-type *E. coli*, such as CM6. However, endogenous pumps can produce significant resistance levels, even in porin-containing cells, under certain conditions. For example, multiple antibiotic resistance (*mar*) mutations in *E. coli* up-regulate a yet-to-be-identified endogenous efflux pump(s) and at the same time down-regulate the expression of OmpF (7), thereby increasing the efficiency of the efflux mechanism. Down-regulation of OmpF occurs under various stress conditions, and perhaps endogenous efflux plays a more important role in the natural environment of gram-negative bacteria than the results obtained with exponential cultures suggest (32).

The proteins catalyzing the endogenous TC efflux in *E. coli* have not been identified, and so we do not know how the direct extrusion of TC into the medium could be achieved. However, many chromosomally coded drug efflux pumps are known to occur together with periplasmic "accessory proteins" or "membrane fusion proteins" (8) which apparently help them in making direct connections to the OM (21, 22, 32). Recently, an operon including a pump, an accessory protein, and a putative OM channel was described in *P. aeruginosa* (39; see also reference 20). It therefore seems plausible that the intrinsic TC efflux pump of *E. coli* would also bypass the outer membrane barrier by a similar mechanism.

ACKNOWLEDGMENTS

We thank Stuart B. Levy and Akira Yamaguchi for the gifts of strains and antiserum, respectively.

This work was supported by NIH grant AI-09644. David Thanassi is a predoctoral trainee supported by NIH training grant GM-07232.

REFERENCES

1. **Albert, A., and C. W. Rees.** 1956. Avidity of the tetracyclines for the cations of metals. Nature (London) **177:**433–434.
2. **Argast, M., and C. F. Beck.** 1985. Tetracycline uptake by susceptible *Escherichia coli* cells. Arch. Microbiol. **141:**260–265.
3. **Bavoil, P., H. Nikaido, and K. von Meyenburg.** 1977. Pleiotropic transport mutants of *Escherichia coli* lack porin, a major outer membrane protein. Mol. Gen. Genet. **158:**23–33.
4. **Bayer, M. H., G. P. Costello, and M. E. Bayer.** 1982. Isolation and partial characterization of membrane vesicles carrying markers of the membrane adhesion sites. J. Bacteriol. **149:**758–767.
5. **Chopra, I., P. M. Hawkey, and M. Hinton.** 1992. Tetracyclines, molecular and clinical aspects. J. Antimicrob. Chemother. **29:**245–277.
6. **Cohen, S. P., H. Hachler, and S. B. Levy.** 1993. Genetic and functional analysis of the multiple antibiotic resistance (*mar*) locus in *Escherichia coli*. J. Bacteriol. **175:**1484–1492.
7. **Cohen, S. P., L. M. McMurry, and S. B. Levy.** 1988. *marA* locus causes decreased expression of OmpF porin in multiple-antibiotic-resistant (Mar) mutants of *Escherichia coli*. J. Bacteriol. **170:**5416–5422.
8. **Dinh, T., I. T. Paulsen, and M. H. Saier, Jr.** 1994. A family of extracytoplasmic proteins that allow transport of large molecules across the outer membranes of gram-negative bacteria. J. Bacteriol. **176:**3825–3831.
9. **Eckert, B., and C. F. Beck.** 1989. Topology of transposon Tn*10*-encoded tetracycline resistance protein within the inner membrane of *Escherichia coli*. J. Biol. Chem. **264:**11663–11670.
10. **Fath, M. J., and R. Kolter.** 1993. ABC transporters: bacterial exporters. Microbiol. Rev. **57:**995–1017.
11. **George, A. M., and S. B. Levy.** 1983. Amplifiable resistance to tetracycline, chloramphenicol, and other antibiotics in *Escherichia coli*: involvement of a non-plasmid-determined efflux of tetracycline. J. Bacteriol. **155:**531–540.
12. **Hansch, C., and A. Leo.** 1979. Substituent constants for correlation analysis in chemistry and biology. John Wiley & Sons, Inc., New York.
13. **Harlow, E., and D. Lane.** 1988. Antibodies: a laboratory manual. Cold Spring Harbor Laboratory, Cold Spring Harbor, N.Y.

14. **Heller, K. B., E. C. C. Lin, and T. H. Wilson.** 1980. Substrate specificity and transport properties of the glycerol facilitator of *Escherichia coli*. J. Bacteriol. **144:**274–278.
15. **Ishidate, K., E. S. Creeger, J. Zrike, S. Deb, B. Glauner, T. J. MacAlister, and L. I. Rothfield.** 1986. Isolation of differentiated membrane domains from *Escherichia coli* and *Salmonella typhimurium*, including a fraction containing attachment sites between the inner and outer membranes and the murein skeleton of the cell envelope. J. Biol. Chem. **261:**428–443.
16. **Jacoby, G. H., and K. D. Young.** 1988. Unequal distribution of penicillin-binding proteins among inner membrane vesicles of *Escherichia coli*. J. Bacteriol. **170:**3660–3667.

16a. **Jogun, K. H., and J. J. Stezowski.** 1976. Chemical-structural properties of tetracycline derivatives. 2. Coordination and conformational aspects of oxytetracycline metal ion complexation. J. Am. Chem. Soc. **98:**6018–6026.

17. **Kashket, E. R.** 1981. Stoichiometry of the H^+-ATPase of growing and resting *Escherichia coli*. Biochemistry **21:**5534–5538.
18. **Levy, S. B.** 1992. Active efflux mechanisms for antimicrobial resistance. Antimicrob. Agents Chemother. **36:**695–703.
19. **Levy, S. B., L. McMurry, P. Onigman, and R. M. Saunders.** 1977. Plasmid-mediated tetracycline resistance in *E. coli*, p. 181–203. *In* J. Drews and G. Hogenauer (ed.), Topics in infectious diseases, vol. 2. R-factors: their properties and possible control. Springer-Verlag, New York.
20. **Li, X.-Z., D. M. Livermore, and H. Nikaido.** 1994. Role of efflux pump(s) in intrinsic resistance of *Pseudomonas aeruginosa*: resistance to tetracycline, chloramphenicol, and norfloxacin. Antimicrob. Agents Chemother. **38:**1732–1741.
21. **Lomovskaya, O., and K. Lewis.** 1992. Emr, an *Escherichia coli* locus for multidrug resistance. Proc. Natl. Acad. Sci. USA **89:**8938–8942.
22. **Ma, D., D. N. Cook, M. Albert, N. G. Pon, H. Nikaido, and J. E. Hearst.** 1993. Molecular cloning and characterization of *acrA* and *acrE* genes of *Escherichia coli*. J. Bacteriol. **175:**6299–6313.
23. **Maloy, S. R., and W. D. Nunn.** 1981. Selection for loss of tetracycline resistance by *Escherichia coli*. J. Bacteriol. **145:**1110–1112.
24. **McMurry, L. M., D. A. Aronson, and S. B. Levy.** 1983. Susceptible *Escherichia coli* cells can actively excrete tetracyclines. Antimicrob. Agents Chemother. **24:**544–551.
25. **McMurry, L. M., J. C. Cullinane, and S. B. Levy.** 1982. Transport of the lipophilic analog minocycline differs from that of tetracycline in susceptible and resistant *Escherichia coli* strains. Antimicrob. Agents Chemother. **22:**791–799.
26. **McMurry, L. M., and S. B. Levy.** 1978. Two transport systems for tetracycline in sensitive *Escherichia coli*: critical role for an initial rapid uptake system insensitive to energy inhibitors. Antimicrob. Agents Chemother. **14:**201–209.
27. **McMurry, L. M., R. E. Petrucci, Jr., and S. B. Levy.** 1980. Active efflux of tetracycline encoded by four genetically different tetracycline resistance determinants in *Escherichia coli*. Proc. Natl. Acad. Sci. USA **77:**3974–3977.
28. **Miller, J. H.** 1972. Experiments in molecular genetics. Cold Spring Harbor Laboratory, Cold Spring Harbor, N.Y.
29. **Muhlradt, P. F., J. Menzel, J. R. Golecki, and V. Speth.** 1974. Lateral mobility and surface density of lipopolysaccharide in the outer membrane of *Salmonella typhimurium*. Eur. J. Biochem. **43:**533–539.
30. **Neidhardt, F. C.** 1987. Chemical composition of *Escherichia coli*, p. 3–6. *In* F. C. Neidhardt, J. L. Ingraham, K. B. Low, B. Magasanik, M. Schaechter, and H. E. Umbarger (ed.), *Escherichia coli* and *Salmonella typhimurium*: cellular and molecular biology, vol. 1. American Society for Microbiology, Washington, D.C.
31. **Nikaido, H.** 1976. Outer membrane of *Salmonella typhimurium*. Transmembrane diffusion of some hydrophobic substances. Biochim. Biophys. Acta **433:**118–132.
32. **Nikaido, H.** 1994. Prevention of drug access to bacterial targets: role of permeability barriers and active efflux. Science **264:**382–388.
33. **Nikaido, H., and E. Y. Rosenberg.** 1981. Effect of solute size on diffusion rates through the transmembrane pores of the outer membrane of *Escherichia coli*. J. Gen. Physiol. **77:**121–135.
34. **Nikaido, H., E. Y. Rosenberg, and J. Foulds.** 1983. Porin channels in *Escherichia coli*: studies with β-lactams in intact cells. J. Bacteriol. **153:**232–240.
35. **Nikaido, H., and D. G. Thanassi.** 1993. Penetration of lipophilic agents with multiple protonation sites into bacterial cells: tetracyclines and fluoroquinolones as examples. Antimicrob. Agents Chemother. **37:**1393–1399.
36. **Nikaido, H., and M. Vaara.** 1985. Molecular basis of bacterial outer membrane permeability. Microbiol. Rev. **49:**1–32.
37. **Osborn, M. J., J. E. Gander, E. Parisi, and J. Carson.** 1972. Mechanism of assembly of the outer membrane of *Salmonella typhimurium*. J. Biol. Chem. **247:**3962–3972.
38. **Plesiat, P., and H. Nikaido.** 1992. Outer membranes of gram-negative bacteria are permeable to steroid probes. Mol. Microbiol. **6:**1323–1333.
39. **Poole, K., K. Krebes, C. McNally, and S. Neshat.** 1993. Multiple antibiotic resistance in *Pseudomonas aeruginosa*: evidence for involvement of an efflux operon. J. Bacteriol. **175:**7363–7372.
40. **Pugsley, A. P., and C. A. Schnaitman.** 1978. Outer membrane proteins of *Escherichia coli*. VII. Evidence that bacteriophage-directed protein 2 functions as a pore. J. Bacteriol. **133:**1181–1189.
41. **Rigler, N. E., S. P. Bag, D. E. Leyden, J. L. Sudmeier, and C. N. Reilley.** 1965. Determination of a protonation scheme of tetracycline using nuclear magnetic resonance. Anal. Chem. **37:**872–875.
42. **Rink, T. J., R. Y. Tsien, and T. Pozzan.** 1982. Cytoplasmic pH and free Mg^{2+} in lymphocytes. J. Cell Biol. **95:**189–196.
43. **Sen, K., J. Hellman, and H. Nikaido.** 1988. Porin channels in intact cells of *Escherichia coli* are not affected by Donnan potentials across the outer membrane. J. Biol. Chem. **263:**1182–1187.
44. **Smit, J., Y. Kamio, and H. Nikaido.** 1975. Outer membrane of *Salmonella typhimurium*: chemical analysis and freeze-fracture studies with lipopolysaccharide mutants. J. Bacteriol. **124:**942–958.
45. **Smith, P. K., R. I. Krohn, G. T. Hermanson, A. K. Mallia, F. H. Gartner, M. D. Provenzano, E. K. Fujimoto, N. M. Goeke, B. J. Olson, and D. C. Klenk.** 1985. Measurement of protein using bicinchoninic acid. Anal. Biochem. **150:**76–85.
46. **Stein, W. D.** 1967. The movement of molecules across cell membranes. Academic Press, Inc., New York.
47. **Stock, J. B., B. Rauch, and S. Roseman.** 1977. Periplasmic space in *Salmonella typhimurium* and *Escherichia coli*. J. Biol. Chem. **252:**7850–7861.
48. **Sugawara, E., and H. Nikaido.** 1992. Pore-forming activity of OmpA protein of *Escherichia coli*. J. Biol. Chem. **267:**2507–2511.
49. **Thanassi, D. G., and H. Nikaido.** Unpublished results.
50. **Witholt, B., M. Boekhout, M. Brock, J. Kingma, H. van Heerikuizen, and L. de Leij.** 1976. An efficient and reproducible procedure for the formation of spheroplasts from variously grown *Escherichia coli*. Anal. Biochem. **74:**160–170.
51. **Yamaguchi, A., K. Adachi, and T. Sawai.** 1990. Orientation of the carboxyl terminus of the transposon Tn*10*-encoded tetracycline resistance protein in *Escherichia coli*. FEBS Lett. **265:**17–19.
52. **Yamaguchi, A., Y. Iwasaki-Ohba, N. Ono, M. Kaneko-Ohdera, and T. Sawai.** 1991. Stoichiometry of metal-tetracycline/H^+ antiport mediated by transposon Tn*10*-encoded tetracycline resistance protein in *Escherichia coli*. FEBS Lett. **282:**415–418.
53. **Yamaguchi, A., T. Udagawa, and T. Sawai.** 1990. Transport of divalent cations with tetracycline as mediated by the transposon Tn*10*-encoded tetracycline resistance protein. J. Biol. Chem. **265:**4809–4813.